2012 American Control Conference
Fairmont Queen Elizabeth, Montréal, Canada
June 27-June 29, 2012

Mathematical Modeling and Fault Detection and Diagnosis of an Electrohydrostatic Actuator

S. Andrew Gadsden, Yu Song, and Saeid R. Habibi, *Member, IEEE*

***Abstract*—This paper studies the mathematical modeling of an electrohydrostatic actuator (EHA) for the purpose of fault detection and diagnosis. A relatively new model-based fault detection strategy referred to as the interacting multiple model and smooth variable structure filtering method (IMM-SVSF) is applied on an experimental apparatus. The results of this application are compared with the popular Kalman filter based strategy (IMM-KF), and recommendations are made for future research.**

I. Introduction

ESTIMATION theory is considered to be a part of signal processing and statistics. It involves finding a value of some parameter of interest, which affects the output of a system, often in the presence of inaccurate or uncertain observations. The purpose of estimation, as described by Bar-Shalom et al. in [1], can be one of many reasons: determination of planet orbit parameters, statistical inference, aircraft traffic control system (i.e., tracking), use in control plants with uncertainties (i.e., parameter identification or state estimation), message retrieval from noisy signals (i.e., communication theory), and also signal and image processing. The ability to successfully control a mechanical or electrical system depends on the knowledge of the true states or parameters of interest. For example, consider a linear mechanical system, where the dynamics such as position, velocity, and acceleration are defined to be the states of interest. The state dynamics, or how the system operates with time, may be captured by using a state representation as follows:

$$x_{k+1} = Ax_k + Bu_k + w_k \tag{1}$$

Where x_k defines the system states, A is the linear system matrix, B is the input gain matrix, u_k is the corresponding input to the system, and w_k refers to the system noise present in the system. To understand the behaviour of a system, elements from the state vector need to be observed or measured. Sensors placed in the environment are used to measure the states of interest. A relationship exists between the measurements and the states, and may be defined as follows:

$$z_{k+1} = Cx_{k+1} + v_{k+1} \tag{2}$$

Manuscript received September 25, 2011. Dr. S. A. Gadsden, Y. Song, and Dr. S. R. Habibi are with the Department of Mechanical Engineering, McMaster University, Hamilton, Ontario, Canada, L8S 4L7 (phone: 905-525-9140; e-mail: gadsdesa@ mcmaster.ca).

Where z_k defines the measurements, C refers to the linear measurement matrix, and v_k refers to the measurement noise present in the sensors. Unless otherwise stated, it is assumed in this paper that the system and measurement noises are modeled as Gaussian noise, with zero mean and covariance's Q_k and R_k, respectively as follows:

$$p(w_k) \sim \mathcal{N}(0, Q_k) \tag{3}$$
$$p(v_k) \sim \mathcal{N}(0, R_k) \tag{4}$$

Therefore, it is the role of a filter to extract knowledge of the true states typically from noisy measurements or observations made of the system, and form state estimates $\hat{x}_k$. The name 'filter' is appropriate since it removes unwanted noise from the signal. Typically, in solving linear estimation problems, the system and measurement dynamics are model based and may be described by discrete-time equations, such as (1) and (2). The concept of filter applies equally well to nonlinear systems and measurements, defined respectively by:

$$x_{k+1} = f(x_k, u_k) + w_k \tag{5}$$
$$z_{k+1} = h(x_{k+1}) + v_{k+1} \tag{6}$$

Where f and h represent the nonlinear system and measurement models, respectively. The most popular and well-studied estimation method is the Kalman filter (KF), which was introduced in the 1960s [2,3]. The KF yields a statistically optimal solution for linear estimation problems, as defined by (1) and (2), in the presence of Gaussian noise. The KF is formulated in a predictor-corrector manner, and is implemented recursively. The optimality of the KF comes at a price of stability and robustness. The KF assumes that the system model is known and linear, the system and measurement noises are zero mean Gaussian, and the states have initial conditions with known means and variances [4,1]. However, the previous assumptions do not always hold in real applications. If these assumptions are violated, the KF may yield suboptimal results and can become unstable [5].

In nature, many systems behave according to a number of different models (modes, or operating regimes). For example, in target tracking, a target may travel straight (i.e., uniform motion) or turn (i.e., undergo a coordinated turn) [1]. Furthermore, a system may experience different types of noises (i.e., white or 'coloured') [6].

978-1-4577-1096-4/12/$26.00 ©2012 AACC

In these scenarios, it is desirable to implement adaptive estimation algorithms, which 'adapt' themselves to certain types of uncertainties or models in an effort to minimize the state estimation error [1]. One type of adaptive estimation technique includes the 'multiple model' (MM) algorithm [7]; which include the following: static MM [8], dynamic MM [1], generalized pseudo-Bayesian (GPB) [9,10,11,12], and the interacting multiple model (IMM) [1,13,14].

For the MM methods, a Bayesian framework is used (i.e., probability based). Essentially, based on some prior probabilities of each model being correct (i.e., the system is behaving according a finite number of modes), the corresponding updated probabilities are calculated [1]. Throughout this paper, it will be assumed that all of the models are linear with the presence of Gaussian noise; however, nonlinear models could be used via linearization [1]. Each MM method requires estimation of the states and their corresponding probability. The most popular strategy that has been implemented in the MM framework remains the KF, and is referred to as the IMM-KF [6]. As such, it forms the basis for comparison in this paper.

II. Smooth Variable Structure Filter

A revised form of the variable structure filter (VSF), referred to as the smooth variable structure filter (SVSF), was presented in 2007 [15]. The SVSF strategy is also a predictor-corrector estimator based on sliding mode concepts, and can be applied on both linear or nonlinear systems and measurements. As shown in the following figure, and similar to the VSF, it utilizes a switching gain to converge the estimates to within a boundary of the true state values (i.e., existence subspace) [15]. The SVSF has been shown to be stable and robust to modeling uncertainties and noise, when given an upper bound on the level of un-modeled dynamics and noise [15,16].

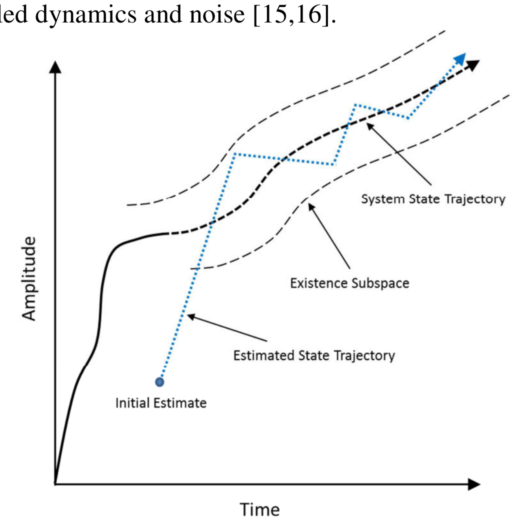

Fig. 1. The SVSF estimation concept is shown here. The SVSF results in the state estimates converging to within an area of the state trajectory, referred to as the existence subspace. Thereafter, it switches back and forth across the state trajectory. The existence subspace represents the amount of uncertainties present in the estimation process, in terms of modeling errors or the presence of noise. Typically this value is not exactly known but an upper bound may be selected based on a priori knowledge.

The origin of the SVSF name comes from the requirement that the system is differentiable (or 'smooth') [15,17]. Furthermore, it is assumed that the system under consideration is observable [15]. Consider the following process for the SVSF estimation strategy, as applied to a nonlinear system with a linear measurement equation. The predicted state estimates $\hat{x}_{k+1|k}$ are first calculated as follows:

$$\hat{x}_{k+1|k} = \hat{f}\left(\hat{x}_{k|k}, u_k\right) \tag{7}$$

Utilizing the predicted state estimates $\hat{x}_{k+1|k}$, the corresponding predicted measurements $\hat{z}_{k+1|k}$ and measurement error vector $e_{z,k+1|k}$ may be calculated:

$$\hat{z}_{k+1|k} = C\hat{x}_{k+1|k} \tag{8}$$

$$e_{z,k+1|k} = z_{k+1} - \hat{z}_{k+1|k} \tag{9}$$

Next, the SVSF gain is calculated as follows [15]:

$$K_{k+1}^{SVSF} = C^{+}\left(\left|e_{z,k+1|k}\right| + \gamma\left|e_{z,k|k}\right|\right) \circ sat\left(\frac{e_{z,k+1|k}}{\psi}\right) \tag{10}$$

The SVSF gain is a function of: the a priori and a posteriori measurement error vectors $e_{z,k+1|k}$ and $e_{z,k|k}$; the smoothing boundary layer widths ψ; the 'SVSF' memory or convergence rate γ with elements $0 < \gamma_{ii} \leq 1$; and the linear measurement matrix C. The SVSF gain is used to refine the state estimates as follows:

$$\hat{x}_{k+1|k+1} = \hat{x}_{k+1|k} + K_{k+1}^{SVSF} \tag{11}$$

Next, the updated measurement estimates $\hat{z}_{k+1|k+1}$ and corresponding errors $e_{z,k+1|k+1}$ are calculated:

$$\hat{z}_{k+1|k+1} = C\hat{x}_{k+1|k+1} \tag{12}$$

$$e_{z,k+1|k+1} = z_{k+1} - \hat{z}_{k+1|k+1} \tag{13}$$

The SVSF process may be summarized by (7) through (13), and is repeated iteratively. According to [15], the estimation process is stable and converges to the existence subspace if the following condition is satisfied:

$$\left|e_{k|k}\right|_{Abs} > \left|e_{k+1|k+1}\right|_{Abs} \tag{14}$$

The proof, as described in [15] and [17], yields the derivation of the SVSF gain from (10).

III. Formulation of the IMM-SVSF

The interacting multiple model (IMM) strategy makes use of a finite number of models, and is associated with filters that run in parallel. The output from each filter includes the state estimate, the covariance, and the likelihood calculation.

The output from the filters is used to calculate mode probabilities, which gives an indication of how close the filter model is to the true model. The IMM has been shown to work significantly better than single model methods, since it is able to make use of more information [1]. It also works extremely well for standard estimation problems such as target tracking, where there are typically two models used to capture the target's trajectory (i.e., uniform motion or coordinated turn) [1].

The motivation for combining the IMM with the SVSF is simple. The SVSF provides an estimation process that is sub-optimal albeit stable. Therefore, utilizing a multiple model (MM) strategy which increases the overall accuracy of the estimation process is beneficial. Furthermore, there was a certain amount of research curiosity present in how the SVSF would perform compared with the KF in terms of model detection probability.

The first step involves calculating the mixing probabilities $\mu_{i|j,k|k}$ (i.e., the probability of the system currently in mode i, and switching to mode j at the next step). These are calculated using the following two equations [1]:

$$\mu_{i|j,k|k} = \frac{1}{\bar{c}_j} p_{ij} \mu_{i,k} \tag{15}$$

$$\bar{c}_j = \sum_{i=1}^{r} p_{ij}\, \mu_{i,k} \tag{16}$$

Recall that p_{ij} refers to the mode transition probabilities, and is a designer parameter. Note that $\mu_{i,k}$ refers to the probability of the mode i being correct (with values between 0 and 1), and differs from the mixing probabilities $\mu_{i|j,k|k}$. This notation is standard, and is found in [1].

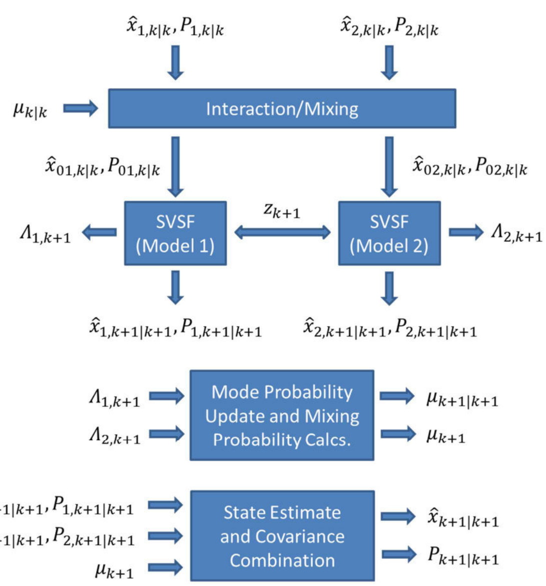

Fig. 2. The IMM-SVSF method is shown here. Essentially, the SVSF estimation strategy may be applied on a finite number of models. As an example, the above figure shows two models. The IMM-SVSF estimator consists of five main steps: calculation of the mixing probabilities, mixing stage, mode-matched filtering via the SVSF, mode probability update, and state estimate and covariance combination.

The mixing probabilities $\mu_{i|j,k|k}$ are used in the mixing stage, next. In addition to the mixing probabilities, the previous mode-matched states $\hat{x}_{i,k|k}$ and covariance's $P_{i,k|k}$ are also used to calculate the mixed initial conditions (states and covariance) for the filter matched to M_j (which consists of A_j and B_j). The mixed initial conditions are found respectively as follows [1]:

$$\hat{x}_{0j,k|k} = \sum_{i=1}^{r} \hat{x}_{i,k|k} \mu_{i|j,k|k} \tag{17}$$

$$P_{0j,k|k} = \sum_{i=1}^{r} \mu_{i|j,k|k} \left\{ P_{i,k|k} + \left(\hat{x}_{i,k|k} - \hat{x}_{0j,k|k}\right)\left(\hat{x}_{i,k|k} - \hat{x}_{0j,k|k}\right)^T \right\} \tag{18}$$

The next step involves mode-matched filtering via the SVSF, which involves using (17) and (18) as inputs to the SVSF matched to M_j. Each SVSF also uses the measurement z_{k+1} and input to the system u_k (if any), and calculates the corresponding updated state estimates (24) and corresponding covariance (25). The state estimates $\hat{x}_{0j,k|k}$ (17) and corresponding covariance $P_{0j,k|k}$ (18) for each model j are used to predict the state estimate $\hat{x}_{j,k+1|k}$ (19) and calculate the a priori state error covariance matrix $P_{j,k+1|k}$ (20).

$$\hat{x}_{j,k+1|k} = A_j \hat{x}_{0j,k|k} + B_j u_k \tag{19}$$

$$P_{j,k+1|k} = A_j P_{k|k}^{0j} A_j^T + Q_k \tag{20}$$

From (19) and (20), the mode-matched innovation covariance $S_{j,k+1|k}$ (21) and mode-matched a priori measurement error $e_{j,z,k+1|k}$ (22) are calculated.

$$S_{j,k+1|k} = C_j P_{j,k+1|k} C_j^T + R_{k+1} \tag{21}$$

$$e_{j,z,k+1|k} = z_{k+1} - C_j \hat{x}_{j,k+1|k} \tag{22}$$

The update stage is defined by the following four equations. The mode-matched SVSF gain $K_{j,k+1}$ is calculated (6.1.9) and used to update the state estimates $\hat{x}_{j,k+1|k+1}$ (6.1.10).

$$K_{j,k+1} = C_j^+ diag\left[\left(\left|e_{j,z,k+1|k}\right| + \gamma_j \left|e_{j,z,k|k}\right|\right) \circ sat\left(\bar{\psi}_j^{-1} e_{j,z,k+1|k}\right)\right] diag\left(e_{j,z,k+1|k}\right)^{-1} \tag{23}$$

$$\hat{x}_{j,k+1|k+1} = \hat{x}_{j,k+1|k} + K_{j,k+1} e_{j,z,k+1|k} \tag{24}$$

The corresponding state error covariance matrix $P_{j,k+1|k+1}$ is then calculated (25) and the a posteriori measurement error $e_{j,z,k+1|k+1}$ may be found (26).

$$P_{j,k+1|k+1} = \left(I - K_{j,k+1} C_j\right) P_{j,k+1|k} \left(I - K_{j,k+1} C_j\right)^T + K_{j,k+1} R_{k+1} K_{j,k+1}^T \tag{25}$$

$$e_{j,z,k+1|k+1} = z_{k+1} - C_j \hat{x}_{j,k+1|k+1} \tag{26}$$

Based on the mode-matched innovation matrix $S_{j,k+1|k}$ (6.1.7) and the mode-matched a priori measurement error $e_{j,z,k+1|k}$ (6.1.8), a corresponding mode-matched likelihood function $\Lambda_{j,k+1}$ based on the SVSF estimation method may be calculated, as follows [1]:

$$\Lambda_{j,k+1} = \mathcal{N}\left(z_{k+1}; \hat{z}_{j,k+1|k}, S_{j,k+1}\right) \tag{27}$$

Equation (6.1.13) may be solved as follows [1,6]:

$$\Lambda_{j,k+1} = \frac{1}{\sqrt{\left|2\pi S_{j,k+1}\right|}} exp\left(\frac{-\frac{1}{2} e_{j,z,k+1|k}^T e_{j,z,k+1|k}}{S_{j,k+1}}\right) \tag{28}$$

Utilizing the mode-matched likelihood functions $\Lambda_{j,k+1}$, the mode probability $\mu_{j,k}$ may be updated by [1]:

$$\mu_{j,k} = \frac{1}{c} \Lambda_{j,k+1} \sum_{i=1}^{r} p_{ij}\, \mu_{i,k} \tag{29}$$

Where the normalizing constant is defined as [1]:

$$c = \sum_{j=1}^{r} \Lambda_{j,k+1} \sum_{i=1}^{r} p_{ij}\, \mu_{i,k} \tag{30}$$

The overall IMM-SVSF state estimates $\hat{x}_{k+1|k+1}$ (31) and corresponding covariance $P_{k+1|k+1}$ (32) are then calculated.

$$\hat{x}_{k+1|k+1} = \sum_{j=1}^{r} \mu_{j,k+1} \hat{x}_{j,k+1|k+1} \tag{31}$$

$$\begin{aligned} P_{k+1|k+1} = \sum_{j=1}^{r} \mu_{j,k+1} \Big\{ & P_{j,k+1|k+1} \\ & + \left(\hat{x}_{j,k+1|k+1} \right. \\ & \left. - \hat{x}_{k+1|k+1}\right)\left(\hat{x}_{j,k+1|k+1} - \hat{x}_{k+1|k+1}\right)^T \Big\} \end{aligned} \tag{32}$$

The formulation of the IMM-SVSF may be summarized by (15) through (32), where there are $i, j = 1, \ldots, r$ models. Note that (31) and (32) are used for output purposes only, and are not part of the algorithm recursions [1]. Furthermore, note that the IMM-KF strategy is the same process as above but (19) through (26) are replaced with the KF prediction and update equations.

IV. Experimental Setup

The experimental setup used in this paper involved an electrohydrostatic actuator (EHA). An EHA is an emerging type of actuator typically used in the aerospace industry. EHAs are self-contained units comprised of their own pump, hydraulic circuit, and actuating cylinder [15]. The main components of an EHA include a variable speed motor, an external gear pump, an accumulator, inner circuitry check valves, and a cylinder (or actuator).

The EHA can be divided into two subsystems. The first is the inner circuit that includes the accumulator and its surrounding check valves. The second is the high pressure outer circuit which performs the actuation. The inner circuit prevents cavitation which occurs when the inlet pressure reaches near vacuum pressures and provides make-up fluid for any dynamic leakage [15]. The following figure shows the experimental setup of the EHA.

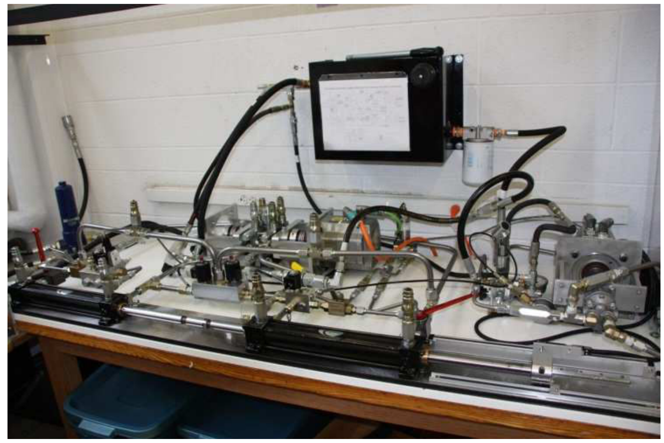

Fig. 3. In the above figure, the cylinder on the right (foreground) is referred to as Axis A and the cylinder connected to it on the left (foreground) is referred to Axis B. An optical linear encoder attached to Axis A is used to obtain position measurements (which are differentiated to obtain velocity measurements). The gear pump and electric motor are located in the rear (middle) of the table.

The electric motor drives the gear pump, which moves the hydraulic fluid throughout the circuit. A voltage input controls the direction and speed of the pump which affects the velocity of the cylinders (or actuators). This setup is a closed hydrostatic circuit [18]. More details on the design and setup of the EHA may be found in [19,20,21,18]. The computer and electrical cabinet are located off-camera to the right of the setup. The software used to communicate with the EHA setup is MATLAB’s Real-Time Windows Target environment.

The two faults that were introduced to the EHA system were increased friction and internal leakage. To incur a friction fault, Axis A was used as the driving mechanism while Axis B acted as a load. To cause internal leakage, the Axis A throttling valve is used (where the Axis A throttle blocking valve is open). As the pump rotates, the Axis A throttling valve incurs cross-port leakage between both chambers of its corresponding cylinder. This action affects the output response of the cylinder.

In order to implement the IMM strategies, three models need to be obtained: normal system operation, and the presence of friction and leakage faults.

V. Mathematical Modeling of the EHA

The EHA may be modeled as a third-order, type 1 linear system with state variables related to its position, velocity, and acceleration. The input to the system is the rotational speed of the pump ω_p, with typical units of rad/s.

In this experimental setup, the sample rate of the system is $T = 1\ ms$. The significant dynamics of the system may be captured by the following third-order transfer function, obtained from [22]:

$$G_{EHA} = \frac{x}{\omega_p} = \frac{EHA_{Num}}{s^3 + EHA_{Den2}s^2 + EHA_{Den1}s} \quad (33)$$

$$EHA_{Num} = \frac{A_E D_P \beta_e}{MV_0} \quad (34)$$

$$EHA_{Den1} = \frac{B_E \beta_e L + A_E^2 \beta_e}{MV_0} \quad (35)$$

$$EHA_{Den2} = \frac{B_E V_0 + M\beta_e L}{MV_0} \quad (36)$$

Note that A_E refers to the piston cross-sectional area, B_E represents the load friction present in the system, β_e is the effective bulk modulus (i.e., the 'stiffness' in the hydraulic circuit), D_p refers to the pump displacement, L represents the leakage coefficient, M is the load mass (i.e., weight of the cylinders), and V_0 is the initial cylinder volume. The three main parameters that affect the EHA model are the pump displacement D_p, load friction B_E, and leakage coefficient L. For the three scenarios (normal, friction, and leakage), these parameters need to be determined in order to correctly mathematically model the EHA system. The following table lists the known EHA parameter values, experimentally determined in [21].

TABLE I
EHA PARAMETER VALUES

Parameter	Physical Significance	EHA Model Values
A_E	Piston Area	$1.52 \times 10^{-3}\ m^2$
D_P	Pump Displacement	$6.876 \times 10^{-7}\ m^3/rad$
M	Load Mass	$7.376\ kg$
V_0	Initial Cylinder Volume	$2.1789 \times 10^{-4}\ m^3$
x_0	Maximum Stroke	$0.14335\ m$
β_e	Effective Bulk Modulus	$2.1 \times 10^8\ Pa$

In an effort to obtain approximate values for the unknown EHA parameters (D_p, B_E, and L), a sequential step signal with amplitude $\pm 2.5\ V$ (changing every 4 seconds) was inputted into the system. Note that this corresponds to a pump rotation of ± 750 RPM. The corresponding (unfiltered) system output is shown in the following figure. Recall that an encoder measured the position of the Axis A cylinder. This value was differentiated to obtain the 'measured' velocity, which resulted in a noisy signal. Note that for the first 12 seconds, the EHA was in normal operation. From 12 seconds to 20 seconds, the EHA experienced the leakage fault. During the final 8 seconds, the friction fault was present.

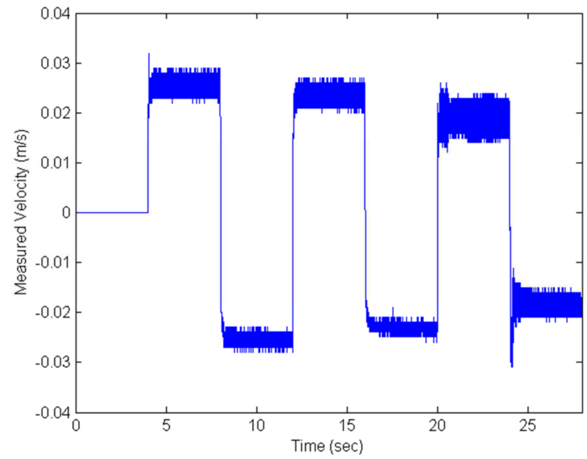

Fig. 4. In the above figure, the unfiltered measured output from the EHA system is shown. Note that for the experimental results, the measurements were digitally filtered to reduce the effects of the noise.

The differential pressure ΔP_A (across the Axis A cylinder) was measured during the data collection for each case. Furthermore, the measured velocity x_∞ (for $+2.5$ V) was averaged for each case, once steady-state was reached (i.e., the final step value). These values, among those found in the previous table, are used to determine the unknown EHA parameters. The first step is to calculate the pump displacement parameter D_p. This can be accomplished using the following formula obtained from [21]:

$$D_p = \frac{Q_E}{\omega_{rad/s}} \quad (37)$$

Essentially (37) defines the pump displacement as a function of volumetric flow rate Q_E and pump turn rate $\omega_{rad/s}$. The volumetric flow rate may be determined from its relationship with pressure, and a series of experimental trials. This relationship is shown in the following figure, as reported in [21].

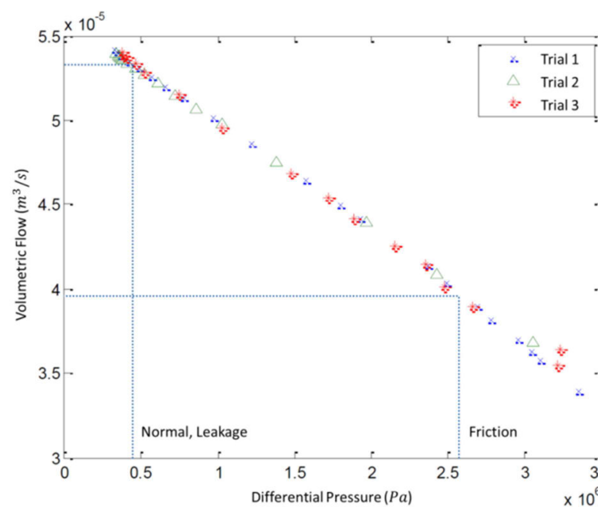

Fig. 5. The above figure shows the relationship between volumetric flow rate and differential pressure [21].

For the normal case, the differential pressure was found to be $70.6\,\text{psi}$ or $486.8\,\text{kPa}$. From the above figure, this results in an approximate volumetric flow rate of $5.35 \times 10^{-5}\,\text{m}^3/\text{s}$. These values result in the following pump displacement, for the normal case:

$$D_p = \frac{(60\,s)\left(5.35 \times 10^{-5}\frac{m^3}{s}\right)}{2\pi(750\,rad)} = 6.812 \times 10^{-7} m^3/rad \tag{38}$$

The pump displacement for the friction and leakage cases may be found in a similar fashion. Next, the load friction B_E will be determined for each scenario. Consider the following equation which simplifies the forces present in the EHA cylinder:

$$F_E = M\ddot{x} + B_E\dot{x} \tag{39}$$

Recall the sequential input to the system as presented earlier. Notice that the measured velocity reaches a steady-state value after a short period of time. At this point, there is no longer acceleration present, such that the force required to overcome friction may be calculated as follows:

$$F_E = \Delta P_A A_E = B_E \dot{x}_\infty \tag{40}$$

Rearranging and simplifying yields:

$$B_E = \frac{\Delta P_A A_E}{\dot{x}_\infty} \tag{41}$$

For the normal case, the averaged steady-state velocity was found to be $0.0259\,\text{m/s}$. Substituting the remaining values into (41) yields the following load friction value for the normal case:

$$B_E = \frac{(486.8 \times 10^3\,Pa)(1.52 \times 10^{-3}\,m^2)}{0.0259\,m/s} = 28{,}569\,Ns/m \tag{42}$$

Finally, the leakage coefficient L may be solved. In order to find an approximate leakage coefficient, consider multiplying the EHA transfer function (33) by s (the Laplace variable), and then solving for L when $s \to 0$. This allows the steady-state value of the velocity $\dot{x}_\infty$ to be used, as follows:

$$\frac{\dot{x}_\infty}{\omega_p} = \frac{EHA_{Num}s}{s^3 + EHA_{Den2}s^2 + EHA_{Den1}s} \tag{43}$$

Then, allowing $s \to 0$ in (43) yields:

$$\left.\frac{EHA_{Num}}{EHA_{Den1}}\right|_{s\to 0} = \dot{x}_\infty = \frac{2.5(10\pi)A_E D_p}{B_E L + A_E^2} \tag{44}$$

Rearranging (44) for the leakage coefficient yields the following:

$$L = \frac{2.5(10\pi)A_E D_p}{B_E \dot{x}_\infty} - \frac{A_E^2}{B_E} \tag{45}$$

Substitution of the known values, as well as (37) and (42), yields:

$$L = \frac{2.5(10\pi)(1.52 \times 10^{-3}\,m^2)(6.812 \times 10^{-7} m^3/rad)}{(28{,}569\,Ns/m)(0.0259\,m/s)} - \frac{(1.52 \times 10^{-3}\,m^2)^2}{28{,}569\,Ns/m} \tag{46}$$

An approximation for the leakage coefficient for the normal case is then found as:

$$L = 2.903 \times 10^{-11}\,Nm/s \tag{47}$$

The above procedures may be repeated for the friction and leakage faults. Finally, based on the aforementioned mathematical modeling, three different transfer functions may be created. The normal model, leakage model, and friction model are respectively defined as follows:

$$G_{EHA,Normal} = \frac{4{,}250}{s^2 + 3{,}901s + 410{,}250} \tag{48}$$

$$G_{EHA,Leakge} = \frac{4{,}250}{s^2 + 4{,}244s + 452{,}160} \tag{49}$$

$$G_{EHA,Friction} = \frac{3{,}138}{s^2 + 27{,}234s + 404{,}370} \tag{50}$$

Note that the EHA system has become a second-order system, where the input is voltage (V), and the output is the cylinder (Axis A) velocity (m/s).

VI. Experimental Results

The results of applying the IMM-SVSF and IMM-KF are provided in this section. Before applying the methods for the purposes of fault detection and diagnosis, the continuous-time transfer functions of (48) through (50) are converted to discrete-time, with $T = 0.001\,s$. The discrete-time transfer functions are then converted to state space representation. The corresponding system and input gain matrices for the normal EHA operation are found as follows:

$$A_{Normal} = \begin{bmatrix} 0.9200 & 1 \\ -0.0202 & 0 \end{bmatrix} \tag{51}$$

$$B_{Normal} = \begin{bmatrix} 7.960 \\ 2.421 \end{bmatrix} \times 10^{-4} \tag{52}$$

The system and input gain matrices for the leakage fault model are determined to be:

$$A_{Leakage} = \begin{bmatrix} 0.9124 & 1 \\ -0.0144 & 0 \end{bmatrix} \tag{53}$$

$$B_{Leakage} = \begin{bmatrix} 7.489 \\ 2.093 \end{bmatrix} \times 10^{-4} \tag{54}$$

Finally, the system and input gain matrices for the friction fault model may be found as follows:

$$A_{Friction} = \begin{bmatrix} 0.9853 & 1 \\ -1.4875 \times 10^{-12} & 0 \end{bmatrix} \quad (55)$$

$$B_{Friction} = \begin{bmatrix} 1.103 \\ 0.042 \end{bmatrix} \times 10^{-4} \quad (56)$$

According to the previous state space models, there are two states. Note that for the purposes of fault detection and diagnosis, the states (whether they are kinematic or not) have no bearing on the results, since one is mainly interested in the mode probability. Only the first state that corresponds to the velocity of the EHA cylinder (Axis A) is measured such that the measurement matrix (used by all three models) is defined as follows:

$$C = [1 \quad 0] \quad (57)$$

For this experimental setup, the system and measurement noise covariance's were defined respectively as follows:

$$Q = \begin{bmatrix} 5 \times 10^{-9} & 0 \\ 0 & 1 \times 10^{-7} \end{bmatrix} \quad (58)$$

$$R = 1.68 \times 10^{-8} \quad (59)$$

The initial state estimates and state error covariance were respectively set to:

$$\hat{x}_{0|0} = [z_0 \quad 0]^T \quad (60)$$

$$P_{0|0} = \begin{bmatrix} 20 & 0 \\ 0 & 20 \end{bmatrix} \quad (61)$$

For the SVSF estimation process, the 'memory' or convergence rate was set to $\gamma = 0.1$, and the smoothing boundary layer widths were defined as $\psi = [0.25 \quad 5]^T$. These parameters were tuned based on minimizing the state estimation error. Furthermore, note that the initial mode probability $\mu_{i,0}$ for both the IMM-KF and IMM-SVSF strategies was set to:

$$\mu_{i,0} = [0.90 \quad 0.05 \quad 0.05] \quad (61)$$

It was assumed with a 90% probability that the EHA experienced normal operation at the start (and a 5% probability for each fault). The mode transition matrix p_{ij} was defined by:

$$p_{ij} = \begin{bmatrix} 0.90 & 0.05 & 0.05 \\ 0.05 & 0.90 & 0.05 \\ 0.05 & 0.05 & 0.90 \end{bmatrix} \quad (62)$$

This matrix is a designer parameter. It states, for example, that there is a 90% probability that the EHA will stay in mode 1 (normal operation) if it was in mode 1 at the current time step (i.e., $p_{11} = 0.90$). It also states that there is a 5% probability that the EHA will move to a different mode.

For the experimental setup, it was assumed that the EHA went under three different mode transitions. For the first 12 seconds, it was operating normally. A leakage fault was then introduced for 8 seconds, followed by a friction fault which also lasted another 8 seconds. Both the IMM-KF and IMM-SVSF strategies were implemented. In the following three figures, a value of '1' refers to a mode probability of 100%, and a value of '0' refers to a mode probability of 0%.

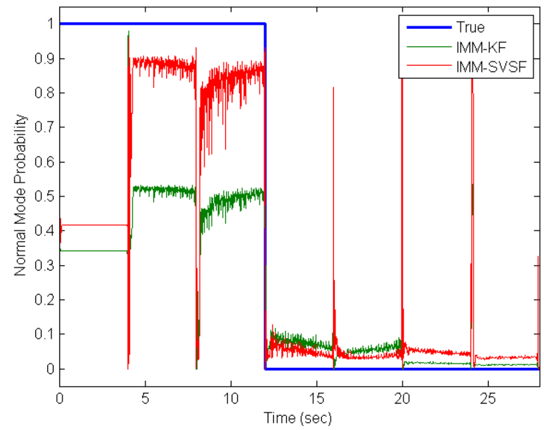

Fig. 6. The above figure shows the normal mode probability for both the IMM-KF and IMM-SVSF methods.

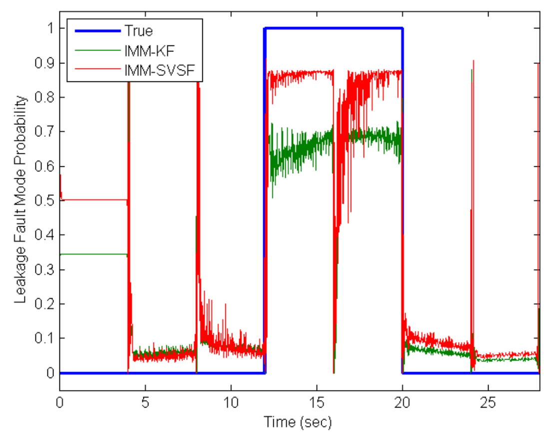

Fig. 7. The above figure shows the leakage mode probability for both the IMM-KF and IMM-SVSF methods.

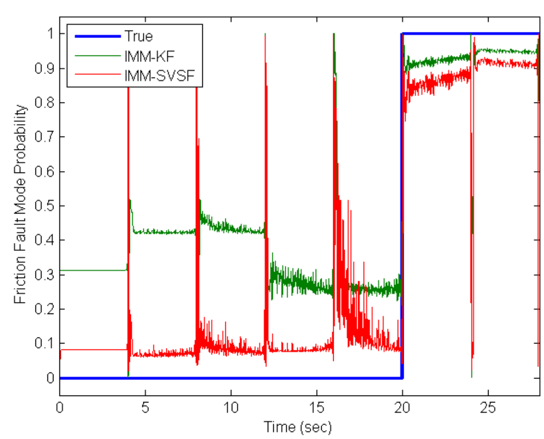

Fig. 8. The above figure shows the friction mode probability for both the IMM-KF and IMM-SVSF methods.

The following tables summarize the averaged mode probability results for this experiment.

TABLE II
IMM-KF AVERAGED MODE PROBABILITY RESULTS

	Normal Detected	Leak Detected	Friction Detected
Normal Present	**48.53** %	8.32 %	43.15 %
Leak Present	6.50 %	**64.46** %	29.04 %
Friction Present	2.25 %	5.31 %	**92.44** %

TABLE III
IMM-SVSF AVERAGED MODE PROBABILITY RESULTS

	Normal Detected	Leak Detected	Friction Detected
Normal Present	**82.70** %	8.48 %	8.82 %
Leak Present	4.83 %	**81.67** %	13.50 %
Friction Present	5.35 %	7.55 %	**87.10** %

Although both strategies worked relatively well, the IMM-KF method had significant difficulty detecting the presence of the friction fault. For example, when the normal mode was present, the IMM-KF correctly identified it with 48.53%; however, it also detected a friction fault with 43.15%. This yields a difference of roughly 5%, which reduces the amount of confidence in correctly identifying the current mode being experienced by the EHA.

The IMM-SVSF strategy was able to correctly detect and diagnosis all three modes with over 80% probability. The IMM-SVSF method outperformed the IMM-KF by 34.17% and 17.21% for the first and second mode, respectively. However, it is interesting to note that the IMM-KF yielded a slightly higher friction detection probability than the IMM-SVSF strategy. It is important to remind the reader that the aforementioned scenarios were specific to a certain linear region in the EHA (at $2.5\,V$), such that the developed mathematical models could be implemented. The actual experimental setup is nonlinear (unmodeled hydraulic dynamics, static friction, and so on) [18]. Developing nonlinear models to fit the entire EHA operating range and then applying the IMM strategies is beyond the scope of this paper.

VII. CONCLUSION

This paper studied the fault detection and diagnosis of an actual EHA built for experimentation. The fault detection case made use of three models: normal system, friction fault, and leakage fault. The models were obtained through mathematically modeling the system. The IMM-SVSF strategy generally outperformed the IMM-KF in terms of estimation accuracy and mode probability determination. Furthermore, the 'false detection' probability was found to be lower for the IMM-SVSF strategy.

REFERENCES

[1] Y. Bar-Shalom, X. Rong Li, and T. Kirubarajan, *Estimation with Applications to Tracking and Navigation*. New York: John Wiley and Sons, Inc., 2001.

[2] R. E. Kalman, "A New Approach to Linear Filtering and Prediction Problems," *Journal of Basic Engineering, Transactions of ASME*, vol. 82, pp. 35-45, 1960.

[3] B. D. O. Anderson and J. B. Moore, *Optimal Filtering*. Englewood Cliffs, NJ: Prentice-Hall, 1979.

[4] D. Simon, *Optimal State Estimation: Kalman, H-Infinity, and Nonlinear Approaches.*: Wiley-Interscience, 2006.

[5] S. J. Julier, J. K. Ulhmann, and H. F. Durrant-Whyte, "A New Method for Nonlinear Transformation of Means and Covariances in Filters and Estimators," *IEEE Transactions on Automatic Control*, vol. 45, pp. 472-482, March 2000.

[6] M. S. Grewal and A. P. Andrews, *Kalman Filtering: Theory and Practice Using MATLAB*, 3rd ed. New York: John Wiley and Sons, Inc., 2008.

[7] X. R. Li, *Advances in Aerospace Systems Dynamics and Control Systems (Volume 76)*, C. T. Leondes, Ed. New York, USA: Academic Press, 1996.

[8] D. T. Magill, "Optimal Adaptive Estimation of Sampled Stochastic Processes," *IEEE Transactions on Automatic Control*, vol. AC-10, pp. 434-439, 1965.

[9] G. A. Ackerson and K. S. Fu, "On State Estimation in Switching Environments," *IEEE Transactions on Automatic Control*, vol. AC-15, no. 1, pp. 10-17, January 1970.

[10] A. G. Jaffer and S. C. Gupta, "Recursive Bayesian Estimation with Uncertain Observation," *IEEE Transactions on Information Theory*, vol. IT-17, pp. 614-616, September 1971.

[11] A. G. Jaffer and S. C. Gupta, "Optimal Sequential Estimation of Discrete Processes with Markov Interrupted Observations," *IEEE Transactions on Automatic Control*, vol. AC-16, pp. 417-475, October 1971.

[12] C. B. Chang and M. Athans, "State Estimation for Discrete Systems with Switching Parameters," *IEEE Transactions on Aerospace and Electronic Systems*, vol. AES-14, no. 5, pp. 418-425, May 1978.

[13] H. A. P. Blom, "An Efficient Filter for Abruptly Changing Systems," in *23rd IEEE Conference on Decision and Control*, Las Vegas, Nevada, December, 1984.

[14] H. A. P. Blom and Y. Bar-Shalom, "The Interacting Multiple Model Algorithm for Systems with Markovian Switching Coefficients," *IEEE Transactions on Automatic Control*, vol. AC-33, no. 8, pp. 780-783, August 1988.

[15] S. R. Habibi, "The Smooth Variable Structure Filter," *Proceedings of the IEEE*, vol. 95, no. 5, pp. 1026-1059, 2007.

[16] S. R. Habibi and R. Burton, "The Variable Structure Filter," *Journal of Dynamic Systems, Measurement, and Control (ASME)*, vol. 125, pp. 287-293, September 2003.

[17] M. Al-Shabi, "The General Toeplitz/Observability SVSF," Department of Mechanical Engineering, McMaster University, Hamilton, Ontario, Ph.D. Thesis 2011.

[18] Y. A. Chinniah, "Fault Detection in the Electrohydraulic Actuator Using the Extended Kalman Filter," Department of Mechanical Engineering, University of Saskatchewan, Saskatoon, Saskatchewan, Ph.D. Thesis 2004.

[19] S. R. Habibi and R. Burton, "Parameter Identification for a High Performance Hydrostatic Actuation System using the Variable Structure Filter Concept," *ASME Journal of Dynamic Systems, Measurement, and Control*, 2007.

[20] M. El Sayed, "Multiple Sliding Mode Control for Electro-Hydraulic Actuation (EHA) Systems," *Article Under Preparation*, 2011.

[21] K. McCullough, "Design and Characterization of a Dual Electro-Hydrostatic Actuator," Department of Mechanical Engineering, McMaster University, Hamilton, Ontario, M.A.Sc. Thesis 2011.

[22] M. El Sayed and S. R. Habibi, "Inner-Loop Control for Electro-Hydraulic Actuation (EHA) Systems," *ASME Journal of Dynamic Systems, Measurement and Control*, 2011 (In Press).